2021 43rd Annual International Conference of the
IEEE Engineering in Medicine & Biology Society (EMBC)
Oct 31 - Nov 4, 2021. Virtual Conference

Multimodal Brain Age Prediction with Feature Selection and Comparison

Bhaskar Ray[1,2], Kuaikuai Duan[1,3], Jiayu Chen[1], Zening Fu[1], Pranav Suresh[1,2], Sarah Johnson[4], Vince D. Calhoun[1,2,3], Jingyu Liu[1,2],

Abstract— **Brain age, an estimated biological age from anatomical and/or functional brain imaging data, and its deviation from the chronological age (brain age gap) have shown the potential to serve as biomarkers for characterizing typical brain development, the abnormal aging process, and early indicators of clinical neuropsychiatric problems. In this study, we leverage multimodal brain imaging data for brain age prediction. We studied and compared the performance of individual data modalities (gray matter density in components and regions of interest, cortical and subcortical anatomical features, resting-state functional connectivity) and different combinations of multiple data modalities using data collected from 1417 participants with age between 8 and 22 years. The result indicates that feature selection and multimodal imaging data can improve brain age prediction with linear support vector and partial least squares regression models. We have achieved a mean absolute error of 1.22 years on the test data with 188 features selected equally from all data sources, better than any individual source. After bias correction, the brain age gap was significantly associated with attention accuracy/speed and motor speed in addition to age. Our results conclude that traditional machine learning with proper feature selection can achieve similar if not better performance compared to complex deep learning neural network methods for the used sample size.**

I. Introduction

Our brain continues to develop and change throughout the lifespan. Neuroimaging data serve as a helpful resource that can be used to study in vivo brain development. Brain age has been recently proposed as one of the biological aging indicators [1] and has been estimated from structural and functional brain imaging data [2,3] in relation to the chronological age of human subjects. The estimated brain age and its divergence from the chronological age have proved to be insightful biomarkers for characterizing typical brain development [1,8], abnormal aging process [4], and early clinical indicators of neuropsychiatric problems [5,9-11].

Multiple brain age models have been published using various features and methods for different age groups [1-4]. Such studies can be characterized as brain age estimations using single or multimodal imaging data with predictions. Some studies used traditional machine learning techniques or new neural network techniques, and some focused on estimates for the brain developmental phase or adulthood.

In the beginning years of brain age research, most models were constructed using regression-based approaches [2-4,6,7]. For instance, based on T1-weighted structural brain imaging of 550 normal subjects aged 19–86, brain age was estimated using relevant vector regression with 410 features extracted by principal component analysis. The accuracy, measured by mean absolute error (MAE), was initially in the 5 year range [2, 7]. Erus et al. studied 621 subjects of ages 8–22 participating in the Philadelphia Neurodevelopmental Cohort (PNC). They applied support vector regression onto 1,116,006 features from multimodal structural imaging maps (gray matter, white matter, ventricular, fractional anisotropy and apparent coefficient of diffusion). They achieved the MAE between the estimated and true age of 1.22 years and reported whole-brain widespread contribution to brain age estimation. These studies, along with others [2,6,7,31], demonstrated that relatively high accuracy of brain age prediction could be achieved by traditional regression methods with a range of MAE between 1 and 5, and multimodal imaging data can result in more accurate brain age estimates than a single imaging modality. However, it is still unclear how the number of features, selection of features, or feature extraction affects brain age estimation accuracy.

Recently neural network-based approaches have been increasingly applied to brain imaging data for brain age prediction [8,12-20]. Cole et al. used a predictive modeling approach based on convolutional neural networks (CNN) on 2001 healthy adults and accurately predicted brain age using gray matter maps (MAE = 4.16 years)[8]. Similarly, the study by M. Ueda et al. used single modality T1 weighted structural MRI data to train a 3D CNN for brain age prediction. This research exhibits that 3D CNN performs better than 2D CNN using a sample size of over 1000 T1-weighted images, resulting in an MAE of 3.67 years [20]. Focused on PNC data, Sturmfels et al. also proposed a novel convolutional neural network (CNN) by adding more filters in the early stage of the architecture for more accurate age prediction (sample size = 1445 T1 weighted structural images and MAE=1.4 years) [19].These studies show that the new deep learning approach can predict brain age with accuracy in the MAE range of between 1 and 4. However, the deep learning approach's strength lies in learning large data, which needs to be further tested for extensive imaging data. [23,32]

Our focus was to further explore the use of multimodal imaging data, including both function and structure, as well

*This work is support by NIH R01DA049238 to VC and JL.

[1]Tri-Institutional Center for Translational Research in Neuroimaging and Data Science (TReNDS), Georgia State University, Georgia Institute of Technology, Emory University, Atlanta, GA, USA. [2]Department of Computer Science, Georgia State University, Atlanta, GA, USA. [3]School of Electrical and Computer Engineering, Georgia Institute of Technology, Atlanta, GA, USA [4]Department of Physics, Georgia State University, Atlanta, GA, USA.

as to evaluate the importance of feature selection for brain age prediction and the number of features necessary for brain age estimation in this study. We analyzed the impact of using different combinations of imaging modalities and their effect on the prediction model. Some studies have used multimodal imaging for brain age prediction. However, to our knowledge, no study has evaluated feature selection or provided an explicit comparison between the different combinations of multimodal data effects on brain age models. Several studies have been conducted using PNC data to predict brain age using either traditional regression methods or a neural network approach. Hence, we also tested our models on PNC data so that our results can be compared with previous works.

II. Materials and Methods

A. Participants and Data

A total of 1598 participants aged 8 to 22 in the PNC recruited from the general population [28] provided multimodal brain imaging data (dbGaP Study Accession: phs000607.v3.p2). PNC study was approved by Institutional Review Board of University of Pennsylvania and the Children's Hospital of Philadelphia. In this study, we analyzed T1 weighted structural MRI (sMRI) and resting-state functional MRI (rs-fMRI). To focus on healthy brain development, we excluded 181 subjects based on gray matter data quality, clinical assessment, and structured interview information. Our final sample consists of 1417 participants (672 male and 745 female, age 13.95 ± 3.57 years old)

B. Gray matter density feature extraction

sMRI images were processed using SPM-12 to generate gray matter maps, including normalization, modulated segmentation with cohort-specific TPM templates, then smoothed by a 6 × 6× 6 mm3 Gaussian kernel. Two different approaches were applied for extracting features from whole-brain gray matter images.

- Independent component analysis (ICA) [30] was applied to estimate 100 independent brain components. The selected 100 ICA components explained a total of 84.76% variance. Loadings of each component represent gray matter network's expression across participants.
- A region of interest (ROI) based approach using the automatic anatomical labeling (AAL) [29] brain atlas extracted 116 brain parcellations. The mean gray matter density of each region was used as the ROI feature.

C. Cortical and subcortical anatomical features

To obtain the brain cortical and subcortical anatomical features we have used the FreeSurfer [26] (version v5.3) software on sMRI images. Estimated total Intracranial volume (eTIV), and cortical thickness, cortical volumes, and subcortical volumes of left and right hemispheres of the brain were extracted to form 152 anatomical features.

D. rs-fMRI functional network connectivity (FNC) features

SPM 12 was used to preprocess all resting-state fMRI scans by performing slice timing correction, realignment, spatial normalization, smoothing steps. Individual's data were removed if more than 30% of frames exceeds 0.3mm framewise displacement, resulting in 1113 subjects for further rs-fMRI analyses. Then we applied group independent component analysis [24] to retrieve the subject-specific brain components. Specifically, we performed two-level PCA deductions with 110 and 100 components and extracted 100 independent brain components. Spatio-temporal regression was used as a back-reconstruction approach to retrieve the subject-specific spatial maps and time courses. After visual inspection, we have selected 56 components as brain functional components. As for post-processing steps on each component's time courses, we performed detrending, despiking, motion correction of 6 motion parameters, bandpass filtering [0.01-0.15 Hz]. Next, we calculated the pairwise Pearson's correlation between time courses as FNCs. The 56 x 56 symmetric matrix was flattened, and a feature vector of size 1540 was extracted from the lower triangle. Next, we applied ICA to the 1113 x 1540 (number of subjects by number of features) FNC features to extract 100 FNC components whose loadings across participants showed individuals FNC expression.

E. Brain age prediction models

For estimation of brain age, we used participants' chronological age as the dependent variable and features derived from brain imaging data as independent predictors. Two different regression models, support vector regression (SVR) with a linear kernel and partial least squares regression, were used in this study. These two regression models were coupled with recursive feature elimination (RFE). RFE is a backward feature elimination approach that assigns a rank to each feature based on its contribution to model prediction accuracy and then eliminates the lower rank features. We divided the samples into 90% training data and 10% testing data. On the training samples, we applied 10-fold cross-validation with the RFE method using SVR estimator to prune the unimportant features. Then the best number of features were selected to achieve the best model parameters. Model input data are from four feature sets to train our brain age prediction model, including 1) Loading of 100 ICA brain components from gray matter images. 2) Gray matter density of 116 AAL regions from gray matter images. 3) 152 brain anatomical features of eTIV, cortical thickness, volume, and subcortical volume measures from sMRI and 4) Loading of 100 FNC components from rs-fMRI FNC vectors. We first tested brain age models with four individual sets of features separately. Then, multimodal brain age prediction was made by various combinations of the four sets of features. The number of subjects varies slightly in different models due to missing data during the data acquisition and feature extraction process.

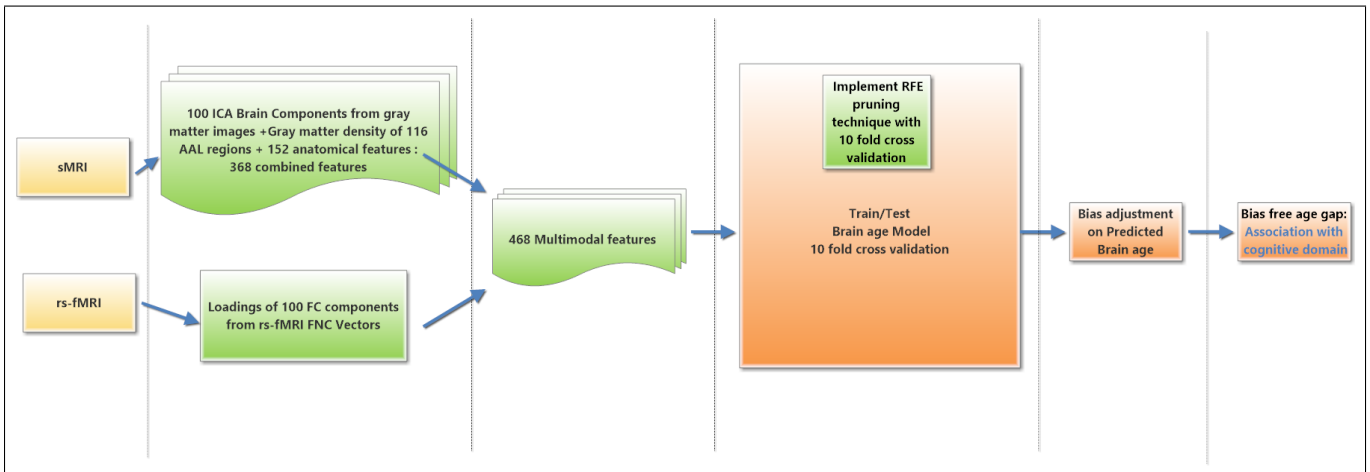

Fig. 1: Overview of the feature extraction and brain age prediction method

F. Training and Testing

- We initially trained two brain age prediction models: support vector regression (linear kernel) and partial least squares regression models, with each of the four individual input datasets in two ways. One is that the full feature space was used for training and testing. The other is that the RFE pruning approach on the individual feature space was applied during training the regression models to reduce the number of features.
- Secondly, we combined all features from brain structure, including 100 ICA gray matter components, 116 AAL ROI gray matter density, and 152 brain anatomical features(a total of 368 brain features), to train our brain age models with and without the RFE pruning.
- Finally, we have combined brain structural and functional features, including the 100 ICA components from FNC derived using rs-fMRI modality, the 100 ICA gray matter components, 116 AAL ROI gray matter density, and 152 brain anatomical features. We trained brain age models with full feature space (a total of 468 features) and RFE pruning on feature space.

G. Bias free brain age difference

We calculated the age gap for each subject by taking the difference between their chronological age and predicted brain age from our best regression model. However, we have observed a negative correlation between the calculated age difference and the individual's chronological age, which indicates that our brain age model's prediction results have some bias due to age dependency. Hence, to achieve a more accurate bias-free estimation from the model, we have implemented the bias reduction technique proposed by Beheshti et al. (2019)[22].

We first calculated the slope and intercept value from the regression line of the brain age gap against each subject's chronological age in this approach. Then we computed an offset value for each sample as follow:

$$Offset = Slope \times Chronological\_age + Intercept \quad (1)$$

Then this offset value is subtracted from the predicted brain age to get the bias-free brain age.

$$Bias\_free\_brain\_age = Estimated\_brain\_age - Offset \quad (2)$$

Finally, we measured the bias-free brain age gap using the subtraction between bias-free brain age and each subject's real age.

H. Comparison with Cognitive domain

We have investigated whether there are any associations between each individual's bias-free brain age gap and their cognitive ability. We performed the n-way analysis of covariance test with the bias-free age difference (continues variable), sex, and chronological age (continuous variable) as independent variables. Dependent variables included the following Computerized Neurocognitive Battery (CNB)[27] test scores: attention (ATT) speed and accuracy, Working memory (WM) speed and accuracy, age-adjusted intelligence quotient (IQ), sensorimotor processing speed (SM), and motor speed (MOT). Each score was tested separately. Finally, we reported adjusted p-values (q-values) by implementing multiple testing corrections with the false discovery rate (FDR) method.

I. Important Brain Regions

To further improve our understanding of the brain age, we highlighted the top 10 features selected by RFE from the final combined datasets just for demonstration purpose. The top 10 features illustrate the brain's top areas that are important for brain age prediction. Then, we plotted all effective brain regions using BrainNetViewer toolbox [25]. All steps in our analyses are summarized in Fig. 1.

TABLE I: Top: MAE of each model on four individual (ICA, AAL, Anatomical and FNC) feature sets without RFE pruning. Bottom: MAE of each model on four individual feature sets with RFE pruning.

Top: Prediction Accuracy on individual datasets (without RFE pruning technique)								
Model /Datasets	Loading of 100 ICA brain components from gray matter images		Gray matter density of 116 AAL regions from gray matter image		152 brain anatomical features from sMRI		Loading of 100 FC components from rs-fMRI FNC vectors.	
	Train (MAE)	Test (MAE)	Train (MAE)	Test (MAE)	Train (MAE)	Test (MAE)	Train (MAE)	Test (MAE)
SVR (Linear Kernel)	1.69 (+/- 0.23)	1.68	1.77 (+/- 0.18)	1.90	1.77 (+/- 0.14)	1.76	1.93 (+/- 0.29)	1.95
PLS	1.69 (+/- 0.22	1.71	1.82 (+/- 0.21)	1.82	1.74 (+/- 0.13)	1.75	1.92 (+/- 0.34)	1.98
Bottom: Prediction Accuracy on individual datasets (with RFE pruning technique)								
Model /Pruned Feature set using RFE method	RFE selected **81** imp ICA components from gray matter images		Gray matter density of RFE selected **70** imp AAL regions		RFE selected **110** imp brain anatomical features		RFE selected **52** imp FC components from rs-fMRI FNC vectors.	
SVR (Linear Kernel)	**1.64 (+/- 0.25)**	**1.60**	1.76 (+/- 0.19)	1.73	1.70 (+/- 0.30)	1.68	1.86 (+/- 0.20)	1.67
PLS	1.68 (+/- 0.23)	1.58	1.78 (+/- 0.20)	1.68	1.72 (+/- 0.31)	1.64	1.86 (+/- 0.23)	1.69

III. Results

A. Prediction ability on individual datasets

We have initially tested our brain age model's performance on the four individual datasets. The brain age estimation error was measured by the mean absolute error (MAE) for each model. Table I lists the MAE during the training and testing for each feature set and for each regression model. (with or without the RFE pruning approach)

We can observe that after removing unimportant features using the RFE technique, the prediction accuracy has slightly increased for all four individual datasets. The 100 ICA brain components feature from gray matter images consistently achieved the best accuracy compared to the other three single-source datasets. From our best-performed model SVR (linear kernel), we got the mean MAE of 1.64 years between predicted brain age and actual age during the training and MAE of 1.60 years during the testing phase with selected 81 important ICA brain components after applying the RFE pruning method.

B. Performance increased with multimodal data

The brain age prediction models were trained with multimodal feature sets using different combinations of the individual sets of features. At first, we aggregated 100 ICA components of gray matter images, gray matter density of 116 AAL regions, and 152 anatomical features to get our first multimodal feature set. We then have added 100 FNC components from resting-state fMRI FNC vector with the first combined dataset to get our second multimodal feature set. The RFE pruning method has selected 120 features from the first multimodal 368 features, and 188 features from the second multimodal 468 features. Multimodal brain age models' performance with and with RFE pruning was listed in Table II.

TABLE II: MAE of each regress model on two multimodal feature sets (with or without RFE pruning).

Model /Datasets	100 ICA brain components & Gray matter density of 116 AAL regions & 152 brain anatomical features: **Total 368 combined features**		100 ICA brain components & Gray matter density of 116 AAL regions & 152 brain anatomical features & 100 FC components: **Total 468 combined features**	
	Train (MAE)	Test (MAE)	Train (MAE)	Test (MAE)
SVR (Linear Kernel)	1.54 (+/- 0.22)	1.32	1.54 (+/- 0.32)	1.67
PLS	1.50 (+/- 0.22)	1.43	1.41 (+/- 0.35)	1.48
Model /Pruned Feature set using RFE method	**Overlapped RFE selected features for both models: (Total: 76)** 100 ICA: 27, 116 AAL ROI: 25, 152 anatomical: 24			
	RFE selected 120, 100 ICA: 40, 116 AAL ROI: 38, 152 anatomical: 42		**RFE Selected 188**, 100 ICA: 41, 116 AAL ROI: 45,152 anatomical: 55, 100 FNC components: 47	
SVR (Linear Kernel)	1.32 (+/- 0.13)	1.25	**1.17 (+/- 0.12)**	**1.22**
PLS	1.40 (+/- 0.13)	1.31	1.26 (+/- 0.11)	1.35

Our prediction result indicates that multimodal data leads to better prediction performance than the unimodal feature sets. The brain age model obtained the best accuracy (MAE 1.17 years during training, MAE 1.22 years during the testing phase) while trained with 188 RFE selected features from the final multimodal dataset. RFE method selected 41 features from 100 ICA gray matter components, 45 features from 116 AAL ROI, 55 features from 152 anatomical features, and 47 features from 100 FNC components to create the final list of 188 useful multimodal feature sets. We can observe that all modalities have almost equal contribution to the final 188 important multimodal feature set.

C. Gender specific model

Gender specific models were also trained with our best performing (RFE selected 188) multimodal feature set. In this approach a male model was trained using only male subjects and a female model was trained with only female subjects.The male model achieved an MAE 1.21 years during training and MAE 1.29 years during test phase from SVR regression model, which is comparable to the accuracy obtained by all subjects together. However, prediction accuracy from the female model was lower since it obtained MAE 1.32 years during training and MAE 1.51 years during testing phase. The male and female models were also compared for predicting age of the opposite sex. Figure 2 plots the actual age against estimated brain age for each gender group. From Figure 2 we can observe that the maturity pace was different for male and female subjects. Also, when female subjects were tested on the male model, the model underestimated ages of females in late adolescence to early adulthood.

D. Bias free Brain age gap

We have used the RFE selected 188 important feature set for computing the brain age difference. Specifically, we retrained our brain age model with a sample size of 1048

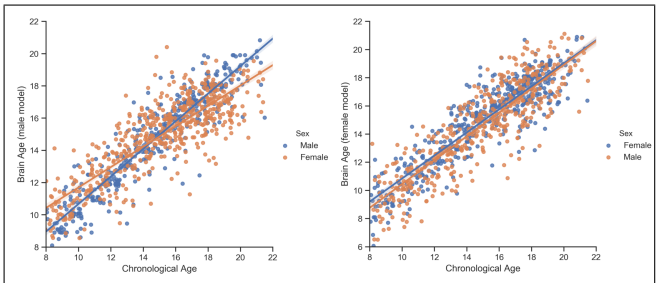

Fig. 2: Scatter plot of chronological age versus brain age on sex specific training models. Blue line indicates training samples, and orange line indicates testing samples.

subjects (subjects had all 188 features). Since we are only using the fixed 188 important features to train our brain age model, the freedom of parameters is also fixed during training. Therefore, we can use more data to get more accurate prediction without facing the overfitting issue. The MAE between predicted and true chronological age was 0.97 years from our best-performed model SVR (linear kernel). After that, we have followed the bias reduction technique proposed by Beheshti et al. (2019)[21] to calculate the bias-free age difference for all subjects.

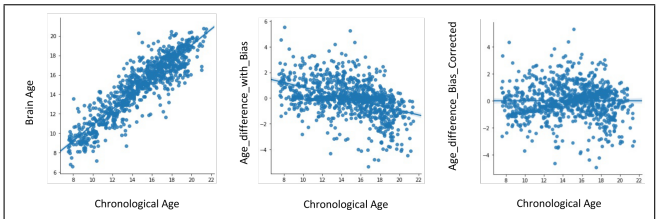

Fig. 3: Left: Scatter plot of predicted brain age vs chronological age (before bias correction) Middle: Scatter plot of estimated brain age difference vs chronological age(before bias correction) Right: Scatter plot of estimated brain age difference vs chronological age(after bias correction)

Figure 3 left plot shows the predicted brain age vs chronological age before we implemented the bias reduction technique. From the middle plot of Figure 3 we can observe a negative relation between brain age difference and chronological age, showing our model overestimated brain age for young children and underestimated brain age for young adults. However, the right plot indicates that the bias got adjusted after implementing the bias correction method.

E. Relationship with cognitive ability

We implemented analyses of co-variance on the seven CNB test sores with the estimated bias-free age gap, sex, and chronological age as independent variables. The significance of the effect from the bias-free brain age gap to each cognitive score was listed in Table III.

Results showed that the bias-free brain age gap significantly affects attention accuracy and speed (ATT accuracy, ATT speed) and motor speed (MOT) of the subjects. We also observed a significant gender effect on the participants'

TABLE III: Significance and effect size of the bias free age gap to seven scores in cognitive domain using analysis of co-variance. Significant values $q \leq 0.05$ after multiple comparison correction are shown in bold.

Cognitive domains	p values	Adjusted p value (q-values)	partial eta-squared (η_p^2)
ATT accuracy	0.02	**0.05**	0.0052
WM accuracy	0.27	0.31	0.0012
SM	0.93	0.93	7.2E-06
IQ	0.11	0.21	0.0025
ATT speed	0.00	**0.01**	0.0096
WM speed	0.16	0.21	0.0019
MOT	0.01	**0.04**	0.0064

attention speed, working memory speed, and motor speed (results not shown here).

F. Plot of effective brain regions

For demonstration purpose we have identified the top 10 regions of the brain that are important for brain age prediction by analyzing the contribution of RFE selected 188 multimodal features. At first, these 188 features were sorted based on the brain age regression model's coefficient value, and then the top 10 (arbitrary choice) features were selected and plotted in Figure 4. Their contribution weights and brain regions are listed in Table IV.

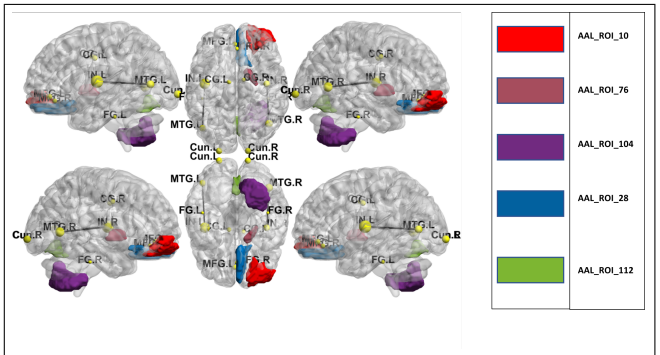

Fig. 4: Top ten effective brain features for age prediction. AAL ROIs are highlighted with different colors. ICA gray matter components are plotted as yellow nodes at the peak voxels. FNC features are shown as edges connecting two yellow nodes.

In Figure 4 the AAL regions were highlighted with different colors, the peak voxels of ICA gray matter components and FNC features were plotted as yellow nodes (with an edge in cases of FNC). By comparing the feature's weight and its brain location from Table IV, we can infer useful information to understand brain development.

IV. Discussion

Our goal in this study is to use a relatively large dataset to investigate brain age prediction performance with single and multiple imaging modalities. We found that SVR (linear kernel) and PLS regression models performed similarly on all single-source feature sets. However, the ICA gray matter components achieved slightly better accuracy compared to any other single-source feature sets in Table I. We also

TABLE IV: Contribution weights and brain location of the top ten features

Feature	Model coefficient	Brain location
AAL_ROI_10	-2.470309	Frontal_Mid_Orb_R
AAL_ROI_76	-2.437359	Pallidum_R
ICA_COMP_78	1.993074	Medial Frontal Gyrus **(MFG)**
ICA_COMP_56	-1.941146	Fusiform Gyrus **(FG)**
ICA_COMP_12	1.894576	Cuneus **(Cun)**
AAL_ROI_104	1.844243	Cerebelum_8_R
AAL_ROI_28	1.798372	Rectus_R
AAL_ROI_112	-1.768712	Vermis_6
ICA_COMP_93	-1.766171	Cingulate Gyrus **(CG)**
FNC_ICA_27	-1.737873	Functional Network Connectivity (FNC) between **Insula & Middle Temporal Gyrus (IN & MTG)**

observed that after pruning the unimportant features using the RFE technique, brain age models showed a little improvement in the prediction performance. The best-performed single-source model (SVR with linear kernel) achieved a MAE of 1.60 years on the test samples while using selected 81 useful features from ICA gray matter data.

When we compared ICA components with averaged gray matter of the corresponding regions, the ICA approach extracted sub-variance of each region, different from simple average. ICA components were more relevant to the age than the simple average of the region which is similar to the ROI-based gray matter density features. Hence, the data-driven variations extracted by ICA presented different and slightly better features than ROIs in age prediction.

When we examined how the brain age models performed if we incorporated multimodal feature sets instead of only one single modality, our analysis results show that the multimodal datasets led to better prediction accuracy. With feature selection, multimodal datasets obtained significantly improved prediction accuracy (improved from MAE 1.60 years to MAE 1.22 years). Our performed two-sample t-test result (t-value: 2.07, p-value: 0.039) indicates that this improved accuracy was statistically significant. The best prediction model was using 188 RFE selected features from the multimodal dataset including all four single modalities. Our best model, SVR (linear kernel), obtained an MAE of 1.22 years on test samples, while it achieved an MAE of 0.97 years from the full samples. No statistical significant differences exist among the coefficients of features of four modalities. Hence, we can say that all unimodal datasets have equally contributed to the final brain age model.

One of the recent studies [19] compared the brain age prediction performance of their proposed convolutional neural networks (CNN) and baseline CNN model on the same PNC dataset (N=1445 sMRI images). Their novel CNN model achieved an MAE of 1.4 years, while the baseline network achieved an MAE of 1.6 years, which are comparable to our results. We have demonstrated that using multimodal pruned important feature sets on traditional machine learning regression methods can achieve similar or better age prediction accuracy instead of other complex approaches like CNN.

We conducted sex-specific training and testing on the brain age models, which show lower prediction accuracy (MAE of 1.51 years on test data) on the all-female model. However, from the male-only model, we got an MAE of 1.29 years during the testing phase, which is in line with the results we got from all subject models. Furthermore, as expected, we found the estimated maturity is different for male and female subjects, consistent with previous work [6].

To understand the meaning of the brain age differences, we calculated a bias-free age gap. We performed an analysis of the covariance test using seven CNB tests as Y (the variable to be predicted) and two continuous variables, age and bias-free age gap, one categorical variable sex as a predictor. As expected, we found that age significantly influenced all seven CNB test variables, indicating cognitive maturity. Also, we observed that sex had shown a significant effect on attention (ATT), working memory (WM), and motor (MOT) speed tests. More importantly, the bias-free brain age gap displayed a significant influence on attention (both speed and accuracy) and motor speed CNB test variables, indicating brain age gap contributes to the individual differences in brain development trajectory and further in the subjects' cognitive maturity.

For illustration purposes, we have plotted the top ten brain features related to brain age prediction. By analyzing the model weights of these ten features, we can figure out the effects of each specific brain location on brain age development. For instance, the top contributor feature ROI-10 has a negative weight (-2.471), which indicates that the gray matter in the middle frontal gyrus will decrease along with the growth of subjects. This may reflect the synaptic pruning process to improve the efficiency of neural transmission. Therefore, with simple linear models, we can explore why a brain region is essential for brain maturity and how that changes over our life span. Compared to the traditional machine learning method using more complex approaches like the deep neural network for brain age prediction, this knowledge will be hard to capture. There have been models that allow for interpreting feature contribution, but these are not as straightforward as linear models.

This study supports the hypothesis of improved brain age prediction accuracy from multimodal data. Our results emphasize that feature selection matters when it comes to brain age prediction accuracy, and only a small set of features are needed. A comparatively simple conventional machine learning approach like SVR can achieve similar or better brain age prediction accuracy as complex approaches such as the convolutional neural network for the used sample size. In the future, we will add more modalities such as genetic information to improve model accuracy and test our

model with an independent dataset to validate the model's generalizability.

REFERENCES

[1] Cole, J. H. and K. Franke (2017). "Predicting Age Using Neuroimaging: Innovative Brain Ageing Biomarkers." Trends Neurosci 40(12): 681-690.

[2] Franke, K., G. Ziegler, S. Kloppel, C. Gaser and I. Alzheimer's Disease Neuroimaging (2010). "Estimating the age of healthy subjects from T1-weighted MRI scans using kernel methods: exploring the influence of various parameters." Neuroimage 50(3): 883-892.3.

[3] Dosenbach, N. U., B. Nardos, A. L. Cohen, D. A. Fair, J. D. Power, J. A. Church, S. M. Nelson, G. S. Wig, A. C. Vogel, C. N. Lessov-Schlaggar, K. A. Barnes, J. W. Dubis, E. Feczko, R. S. Coalson, J. R. Pruett, Jr., D. M. Barch, S. E. Petersen and B. L. Schlaggar (2010). "Prediction of individual brain maturity using fMRI." Science 329(5997): 1358-1361.

[4] Cole, J. H., S. J. Ritchie, M. E. Bastin, M. C. Valdes Hernandez, S. Munoz Maniega, N. Royle, J. Corley, A. Pattie, S. E. Harris, Q. Zhang, N. R. Wray, P. Redmond, R. E. Marioni, J. M. Starr, S. R. Cox, J. M. Wardlaw, D. J. Sharp and I. J. Deary (2018). "Brain age predicts mortality." Mol Psychiatry 23(5): 1385-1392.

[5] Kaufmann, T., D. Alnaes, N. T. Doan, C. L. Brandt, O. A. Andreassen and L. T. Westlye (2017). "Delayed stabilization and individualization in connectome development are related to psychiatric disorders." Nat Neurosci 20(4): 513-515.

[6] Erus, G., H. Battapady, T. D. Satterthwaite, H. Hakonarson, R. E. Gur, C. Davatzikos and R. C. Gur (2015). "Imaging patterns of brain development and their relationship to cognition." Cereb Cortex 25(6): 1676-1684..

[7] Franke, K., E. Luders, A. May, M. Wilke and C. Gaser (2012). "Brain maturation: predicting individual BrainAGE in children and adolescents using structural MRI." Neuroimage 63(3): 1305-1312.

[8] Cole, J. H., R. P. K. Poudel, D. Tsagkrasoulis, M. W. A. Caan, C. Steves, T. D. Spector and G. Montana (2017). "Predicting brain age with deep learning from raw imaging data results in a reliable and heritable biomarker." Neuroimage 163: 115-124.

[9] Liang, H., F. Zhang and X. Niu (2019). "Investigating systematic bias in brain age estimation with application to post-traumatic stress disorders." Hum Brain Mapp 40(11): 3143-3152.

[10] Beheshti, I., S. Mishra, D. Sone, P. Khanna and H. Matsuda (2020). "T1-weighted MRI-driven Brain Age Estimation in Alzheimer's Disease and Parkinson's Disease." Aging Dis 11(3): 618-628.

[11] Egorova, N., F. Liem, V. Hachinski and A. Brodtmann (2019). "Predicted Brain Age After Stroke." Front Aging Neurosci 11: 348.

[12] Peng, H., W. Gong, C. F. Beckmann, A. Vedaldi and S. M. Smith (2021). "Accurate brain age prediction with lightweight deep neural networks." Med Image Anal 68: 101871.

[13] Hong, J., Z. Feng, S. H. Wang, A. Peet, Y. D. Zhang, Y. Sun and M. Yang (2020). "Brain Age Prediction of Children Using Routine Brain MR Images via Deep Learning." Front Neurol 11: 584682.

[14] Feng, X., Z. C. Lipton, J. Yang, S. A. Small, F. A. Provenzano, I. Alzheimer's Disease Neuroimaging, B. Australian Imaging, a. Lifestyle flagship study of and I. Frontotemporal Lobar Degeneration Neuroimaging (2020). "Estimating brain age based on a uniform healthy population with deep learning and structural magnetic resonance imaging." Neurobiol Aging 91: 15-25.

[15] Jonsson, B. A., G. Bjornsdottir, T. E. Thorgeirsson, L. M. Ellingsen, G. B. Walters, D. F. Gudbjartsson, H. Stefansson, K. Stefansson and M. O. Ulfarsson (2019). "Brain age prediction using deep learning uncovers associated sequence variants." Nat Commun 10(1): 5409.

[16] Bermudez, C., A. J. Plassard, S. Chaganti, Y. Huo, K. S. Aboud, L. E. Cutting, S. M. Resnick and B. A. Landman (2019). "Anatomical context improves deep learning on the brain age estimation task." Magn Reson Imaging 62: 70-77.

[17] Amoroso, N., M. La Rocca, L. Bellantuono, D. Diacono, A. Fanizzi, E. Lella, A. Lombardi, T. Maggipinto, A. Monaco, S. Tangaro and R. Bellotti (2019). "Deep Learning and Multiplex Networks for Accurate Modeling of Brain Age." Front Aging Neurosci 11: 115.

[18] Schulz, M. A., B. T. T. Yeo, J. T. Vogelstein, J. Mourao-Miranada, J. N. Kather, K. Kording, B. Richards and D. Bzdok (2020). "Different scaling of linear models and deep learning in UKBiobank brain images versus machine-learning datasets." Nat Commun 11(1): 4238.

[19] Sturmfels, P., Rutherford, S., Angstadt, M., Peterson, M., Sripada, C., & Wiens, J. (2018). A Domain Guided CNN Architecture for Predicting Age from Structural Brain Images. MLHC.

[20] M. Ueda et al., "An Age Estimation Method Using 3D-CNN From Brain MRI Images," 2019 IEEE 16th International Symposium on Biomedical Imaging (ISBI 2019), Venice, Italy, 2019, pp. 380-383, doi: 10.1109/ISBI.2019.8759392.

[21] Beheshti, I., S. Nugent, O. Potvin and S. Duchesne (2019). "Bias-adjustment in neuroimaging-based brain age frameworks: A robust scheme." Neuroimage Clin 24: 102063.

[22] Smith, S. M., D. Vidaurre, F. Alfaro-Almagro, T. E. Nichols and K. L. Miller (2019). "Estimation of brain age delta from brain imaging." Neuroimage 200: 528-539.

[23] Schulz, M. A., B. T. T. Yeo, J. T. Vogelstein, J. Mourao-Miranada, J. N. Kather, K. Kording, B. Richards and D. Bzdok (2020). "Different scaling of linear models and deep learning in UKBiobank brain images versus machine-learning datasets." Nat Commun 11(1): 4238.

[24] Calhoun, V. D., T. Adali and J. J. Pekar (2004). "A method for comparing group fMRI data using independent component analysis: application to visual, motor and visuomotor tasks." Magn Reson Imaging 22(9): 1181-1191.

[25] Xia, M., J. Wang and Y. He (2013). "BrainNet Viewer: a network visualization tool for human brain connectomics." PLoS One 8(7): e68910.

[26] Khan, A. R., L. Wang and M. F. Beg (2008). "FreeSurfer-initiated fully-automated subcortical brain segmentation in MRI using Large Deformation Diffeomorphic Metric Mapping." Neuroimage 41(3): 735-746.

[27] Gur, R. C., Richard, J., Calkins, M. E., Chiavacci, R., Hansen, J. A., Bilker, W. B., Loughead, J., Connolly, J. J., Qiu, H., Mentch, F. D., Abou-Sleiman, P. M., Hakonarson, H., & Gur, R. E. (2012). Age group and sex differences in performance on a computerized neurocognitive battery in children age 8-21. Neuropsychology, 26(2), 251–265. https://doi.org/10.1037/a0026712

[28] Satterthwaite, T. D., Connolly, J. J., Ruparel, K., Calkins, M. E., Jackson, C., Elliott, M. A., Roalf, D. R., Hopson, R., Prabhakaran, K., Behr, M., Qiu, H., Mentch, F. D., Chiavacci, R., Sleiman, P., Gur, R. C., Hakonarson, H., & Gur, R. E. (2016). The Philadelphia Neurodevelopmental Cohort: A publicly available resource for the study of normal and abnormal brain development in youth. NeuroImage, 124(Pt B), 1115–1119. https://doi.org/10.1016/j.neuroimage.2015.03.056

[29] Rolls, E. T., C. C. Huang, C. P. Lin, J. Feng and M. Joliot (2020). "Automated anatomical labelling atlas 3." Neuroimage 206: 116189.

[30] Xu, L., Groth, K. M., Pearlson, G., Schretlen, D. J., & Calhoun, V. D. (2009). Source-based morphometry: the use of independent component analysis to identify gray matter differences with application to schizophrenia. Human brain mapping, 30(3), 711–724. https://doi.org/10.1002/hbm.20540

[31] Liem, F., Varoquaux, G., Kynast, J., Beyer, F., Kharabian Masouleh, S., Huntenburg, J. M., Lampe, L., Rahim, M., Abraham, A., Craddock, R. C., Riedel-Heller, S., Luck, T., Loeffler, M., Schroeter, M. L., Witte, A. V., Villringer, A., & Margulies, D. S. (2017). Predicting brain-age from multimodal imaging data captures cognitive impairment. NeuroImage, 148, 179–188. https://doi.org/10.1016/j.neuroimage.2016.11.005

[32] Abrol, A., Fu, Z., Salman, M., Silva, R., Du, Y., Plis, S., & Calhoun, V. (2020). Hype versus hope: Deep learning encodes more predictive and robust brain imaging representations than standard machine learning. bioRxiv.